JOURNAL OF THE AMERICAN WATER RESOURCES ASSOCIATION

AMERICAN WATER RESOURCES ASSOCIATION

THE SHALLOW-WATER COMPONENT OF THE CHESAPEAKE BAY ENVIRONMENTAL MODEL PACKAGE[1]

Carl F. Cerco, Mark R. Noel, and Ping Wang[2]

ABSTRACT: The shallow-water component of the Chesapeake Bay Environmental Model Package emphasizes the regions of the system inside the 2-m depth contour. The model of these regions is unified with the system-wide model but places emphasis on locally significant components and processes, notably submerged aquatic vegetation (SAV), sediment resuspension, and their interaction with light attenuation (Ke). The SAV model is found to be most suited for computing the equilibrium distribution of perennial species. Addition of plant structure and propagation are recommended to improve representation of observed trends in SAV area. Two approaches are taken to examining shallow-water Ke. The first compares observed and computed differences between deep- and shallow-water Ke. No consistent difference in observations is noted. In the preponderance of regions examined, computed shallow-water Ke exceeds computed deep-water Ke. The second approach directly compares Ke measured in shallow water with modeled results. Model values are primarily lower than observed, in contrast to results in deep water where model values exceed observed. The shortfall in computed Ke mirrors a similar shortfall in computed suspended solids. Improved model representation of Ke requires process-based investigations into suspended solids dynamics as well as increased model resolution in shallow-water regions.

(KEY TERMS: turbidity; macrophytes; sediment transport; eutrophication; simulation; Chesapeake Bay.)

Cerco, Carl F., Mark R. Noel, and Ping Wang, 2013. The Shallow-Water Component of the Chesapeake Bay Environmental Model Package. *Journal of the American Water Resources Association* (JAWRA) 1-12. DOI: 10.1111/jawr.12106

INTRODUCTION

The spatial resolution of Chesapeake Bay management models has been subject to continuous revision since the beginning of the modern management era, circa 1985. The present combined hydrodynamic/eutrophication models have moved from an initial computational grid of 729 surface elements ($\approx$2.8 $\times$ 5.6 km) (Johnson *et al.*, 1993; Cerco and Cole, 1993) to the present grid of more than 11,000 surface elements ($\approx$1 $\times$ 1 km) (Kim, this issue; Cerco and Noel, this issue). Minimum depth represented has been reduced from 3.3 to 2.1 m. The objective of the increased resolution was to move the model domain into regions of smaller spatial extent and less depth. The improved resolution of the present model was intended, in part, to facilitate use of the model in examining attainment of water quality criteria in "shallow-water bay grass designated use" regions (USEPA, 2003). The criteria are based on area covered by submerged aquatic vegetation (SAV), on area meeting criteria for light attenuation (Ke), or on combinations of these two areas within 92 regions designated

[1]Paper No. JAWRA-12-0064-P of the *Journal of the American Water Resources Association* (JAWRA). Received March 13, 2012; accepted September 8, 2012.

[2]Respectively, Research Hydrologist (Cerco) and Mathematician (Noel), US Army Engineer Research and Development Center, 3909 Halls Ferry Road, Vicksburg, Mississippi 39180; Senior Research Scientist (Wang), Virginia Institute of Marine Science Chesapeake Bay Office, Annapolis, Maryland (E-Mail/Cerco: carl.f.cerco@usace.army.mil).

as Chesapeake Bay Program Segments (CBPS) (USEPA, 2008). We describe here the shallow-water components of the Chesapeake Bay Environmental Model Package (CBEMP) and present results with emphasis on SAV and Ke. Shallow water is defined as the area within the 2-m depth contour (Figure 1). This depth is the outer limit of targeted SAV restoration (USEPA, 2003) and coincides with the minimum depth resolution of the present computational grid. As with our report on the 21-year simulation (Cerco and Noel, this issue), we restrict attention to the mainstem of the bay and adjacent embayments. Results for western tributaries are found in Cerco *et al.* (2010).

FIGURE 1. Chesapeake Bay Model Domain, Showing Shallow-Water Regions (Depth ≤ 2 m).

METHODS

The Shallow-Water Model

Shallow-water model segments form a ribbon around the perimeter of the modeled region (Figure 1), augmented by additional shallow areas at the heads of tributaries and embayments. The shallow-water model (Figure 2) is an integral part of the larger Corps of Engineers Integrated Compartment Water Quality Model (CE-QUAL-ICM) representation of Chesapeake Bay (Cerco and Noel, this issue; Cerco *et al.*, 2010). The sole model component unique to shallow water is the SAV model. Otherwise, the model features are the same although the relative importance of various components and processes may be different from the relative importance in deeper, open water. Transport processes, including exchange with regions of greater depth, are computed by the CH3D hydrodynamic model (Kim, this issue). Computational elements (or cells) that adjoin the shoreline receive nutrient and sediment loads from the adjacent watershed (Shenk and Linker, this issue) and from shoreline erosion (Cerco *et al.*, 2010). Sediment resuspension is computed based on shear stress generated from currents and waves (Cerco *et al.*, 2010). Diagenetic processes are computed by a sediment diagenesis model (DiToro, 2001). Activity of bivalve filter feeders is computed by a filter-feeder module (Cerco and Noel, 2010). Oysters are the dominant modeled bivalve in saline water and the potential for oyster restoration to remediate eutrophication has been previously considered (Cerco and Noel, 2007). Oyster restoration is not an element of the present Total Maximum Daily Load (TMDL), however, and the influence of the existing, depleted, population on water quality is minimal. Consequently, oysters are not considered herein.

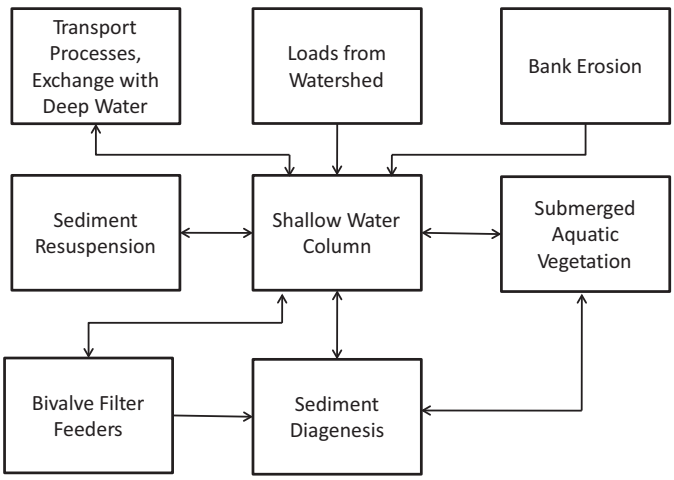

FIGURE 2. Schematic Representation of the Shallow-Water Model.

The model was initially calibrated to the period 1993-1999 with a subsequent extension to the years 1985-2005. In addition to the calibration, several sensitivity runs were conducted to examine the influence of parameter values and forcing functions on calculated values. Sensitivity runs included the following: (1) no solids loads from the watershed; (2)

no solids loads from bank erosion; (3) reduce solids settling velocity; and (4) eliminate feedback between SAV and bottom shear stress.

SAV Model Refinements

The basic SAV unit model is retained from previous applications (Cerco and Moore, 2001). State variables include above-ground biomass (g C m^{-2}), below-ground biomass (g C m^{-2}), and epiphytes (g C/g leaf C). The unit model operates on an independent SAV sub-grid (Figure 3), however, rather than on the hydrodynamic model computational grid, as considered previously. The sub-grid is designed to alleviate two difficulties with previous model applications: spatial resolution and model-data comparisons.

The spatial extent of SAV beds can be smaller than practical computational cells while bathymetry variations that determine bed extent may be too small to represent on the most highly resolved grids. In the Chesapeake, the maximum depth of SAV beds is less than 2 m and bathymetry variations of 10-20 cm can differentiate between the highest density SAV and virtually no SAV. However, computational cells in regions that support SAV are 2 m deep at mean tide and the depth is uniform within each cell.

The gap between spatial scales is bridged by adapting an SAV sub-grid. Computational grid cells are linked to SAV grid cells, which are divided into multiple depth increments. Conditions in the water column and sediments on the SAV grid are obtained from the larger grid. Light available to SAV and the resulting SAV biomass are computed for each depth increment (0-0.5 m, 0.5-1.0 m, 1.0-1.5 m, 1.5-2.0 m) on the sub-grid. The area encompassed by each depth increment is determined from bathymetry and from observed SAV extent. Mass balance is maintained by accounting for the area represented by each SAV depth increment. Areal mass fluxes between SAV and water or sediments in SAV grid cells are multiplied by the area of each local depth increment, summed over all depth increments, and then communicated to corresponding cells on the larger model grid in units of mass per time.

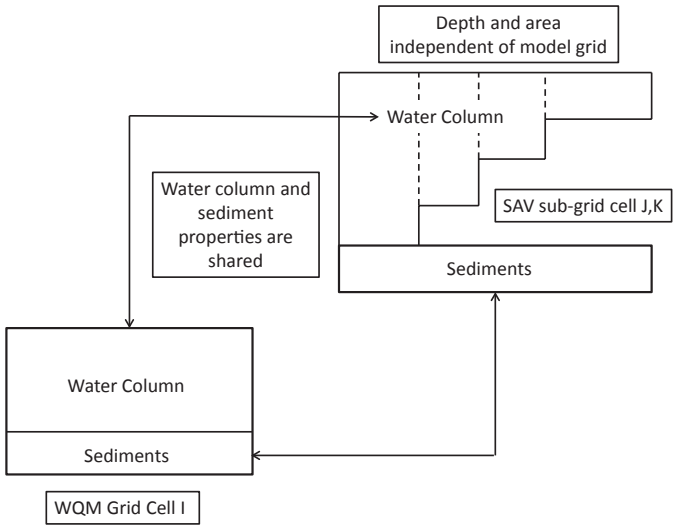

FIGURE 3. The Submerged Aquatic Vegetation (SAV) Sub-Grid. Computed conditions in the water and sediments of a cell in the system-wide computational grid are shared with the corresponding cell on the SAV sub-grid. The SAV sub-grid is divided into multiple depth increments to provide more detailed spatial resolution of light available to SAV than is possible in one cell of the system-wide grid. Mass fluxes between SAV and the surroundings computed on the sub-grid are transmitted to the system-wide grid and included in mass balance calculations.

Another advantage of the sub-grid is the area of SAV beds is quantifiable within the model. SAV occupies cells, and depth increments within cells, depending largely on computed irradiance. Summation of the populated cell areas within each CBPS allows direct comparison with the SAV areas observed in annual overflights. Previously, the observed SAV area had to be converted to biomass for comparison with the model.

The initial comparisons of computed and observed SAV area inevitably showed computed areas in excess of observed. We suspected the problem originated with factors that influence SAV growth but were not considered in the model, especially reproduction and propagation. Consequently, the concept of "probability of growth" was introduced (Cerco *et al.*, 2010). The major purpose of introducing probability was to limit SAV production even though habitat criteria for light were fulfilled. Probability in any growing season was linked to the existence of SAV above a threshold biomass in the previous growing season. Our hypothesis was that the existence of SAV promotes propagation by providing seeds and tubers and through amelioration of ambient conditions, e.g., damping of solids resuspension.

The probability algorithm was accessed on January 1 of each model year for each SAV cell and depth increment. If SAV density exceeded a threshold, the model proceeded. If density was below the threshold, the probability of success was determined from a random number generator. If the random number fell within a specified range, the model proceeded. Otherwise, no growth occurred for that year.

Light Attenuation from Inherent Optical Properties

Light attenuation in previous model versions was computed by a "partial attenuation model" in which Ke was computed as the sum of contributions from water, volatile solids, and fixed solids (Cerco and Noel, 2004). Parameters in the partial attenuation model were determined by linear regression of observed Ke against

observed solids concentrations and adjusted to maximize agreement between computed and observed Ke. For this application, the calculation of Ke is based on inherent optical properties including color, absorption, and scattering (Lee *et al.*, 2005; Gallegos *et al.*, 2011). Color and parameters which relate absorption and scattering to chlorophyll and suspended solids are based, to the greatest extent possible, on field observations (Gallegos *et al.*, 2006). Implementation of the revised light attenuation calculation requires solution of more than 20 equations. Solution of the full suite of equations at each model time step for every cell presents a prohibitive computational burden, which is eliminated through use of a lookup table. An array of 2,000,000 simulated values of Ke is generated, based on nested loops of the following six independent variates: colored dissolved organic matter, phytoplankton absorption, particulate scattering, non-algal particulate absorption, solar zenith angle, and backscatter fraction. The lookup table is expressed as a FORTRAN subroutine that is incorporated into the eutrophication model. At each time iteration and grid location, the eutrophication model provides day of year, computed chlorophyll concentration, and computed total suspended solids (TSS) to the subroutine. The subroutine computes six independent variates from the model values and returns Ke determined from the lookup table.

Observed SAV Areas

Submerged aquatic vegetation is surveyed once annually via aerial overflights and reported as bed area in each of the CBPS. The areas for the model application period, 1985-2005, were obtained from an on-line database (Virginia Institute of Marine Science, SAV in Chesapeake Bay. Accessed December 12, 2011, http://web.vims.edu/bio/sav/SegmentArea Table.htm) and prepared as time series for comparison with the model in each CBPS. A time series of annual bay-wide sums was also prepared. Model areas, for comparison with observed, were taken as the sum of SAV sub-grid areas with computed SAV biomass in excess of a threshold value, 10 g leaf C m^{-2}. The threshold was a minimum model value maintained in each grid element as a "seed" population.

Observed Shallow-Water Light Attenuation

The Chesapeake Bay Program and its partners operate an extensive multi-faceted monitoring program (Chesapeake Bay Program Data Hub. Accessed December 12, 2011, http://www.chesapeakebay.net/dataandtools.aspx). Water quality monitoring at more than 90 stations throughout the system commenced in mid-1984. Location of these stations is permanent and they are concentrated in channels and in open water. Light attenuation is obtained via conversion from disk visibility (Holmes, 1970) or derived from measures of downwelling irradiance *vs.* depth. Operation of a shallow-water monitoring system (Maryland DNR, Eyes on the Bay. Accessed December 12, 2011, http://mddnr.chesapeakebay.net/eyesonthebay/Publications.cfm), aimed at monitoring attainment of relevant water quality criteria, commenced in 1998. Observations are sparse, however, before 2002. In this system, light attenuation is predominantly measured as turbidity and converted to attenuation through regression relationships determined for local conditions (USEPA, 2008). The measurement protocol combines fixed stations and continuous observations from moving vessels. The fixed stations are not permanent, but rotate every three years to provide coverage of the extensive shallow-water regions. The shallow-water monitoring data are outside the initial model calibration period of 1993-1999. To use the data initially, a scheme was devised which compared model mean values at channel stations and shallow-water stations, over the calibration period, with mean observed values in the channel and shallow water collected circa 2002-2005. The scheme aimed, as well, to compare modeled differences between deep and shallow water with observed differences. Observations from 34 fixed shallow-water stations were paired with adjacent channel stations. The pairing matched turbidity measured in shallow water with attenuation measured in the channel at the same time. The database was restricted to shallow stations which could be paired with at least 10 independent observations at a channel station. Shallow-water turbidity measures were converted to attenuation using regression relationships (USEPA, 2008).

Light attenuation, derived from measures of irradiance *vs.* depth, is measured at fixed shallow-water stations at intervals when the instruments are serviced. Samples are also collected for analyses of various constituents including TSS and chlorophyll. When the model application period was extended to 2005 (Cerco and Noel, this issue), attenuation and associated observations at 62 shallow-water stations were obtained and mapped to the model grid (Figure 4) for direct comparison with computations.

RESULTS

SAV Model

The SAV model considers three exclusive communities: FRESHWATER, RUPPIA, ZOSTERA (Moore

FIGURE 4. Shallow-Water Monitoring Stations. Deep- and shallow-water station pairs (comparison) are shown as well as stations used in exact comparison with model computations.

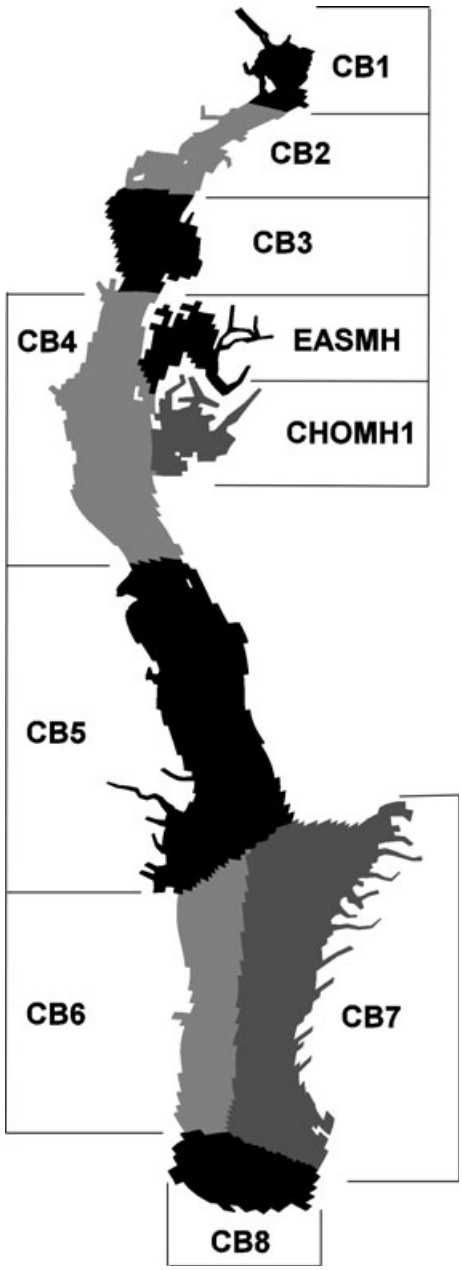

FIGURE 5. Chesapeake Bay Program Segments Employed to Calibrate Submerged Aquatic Vegetation Model and in Examination of Computed Deep- *vs.* Shallow-Water Light Attenuation.

et al., 2000; Cerco and Moore, 2001). A community is assigned to a model cell based on the observed distribution and on environmental characteristics, especially salinity. Parameters for each community are largely as in the original model, with adjustments as necessary. Derivation of the final parameter set (Cerco *et al.*, 2010) followed the original pattern. The unit model was parameterized to replicate observed intra-annual SAV biomass from an assembly of observations. The unit model was next installed in the larger system-wide model and SAV computations in selected segments (Figure 5) were checked against habitat criteria for light (Chesapeake Bay Program, 1992). The segments were selected based on abundance of SAV and availability of ancillary data for calibration and verification.

Observed system-wide SAV area over the interval 1985-2005 more than doubled (Figure 6), largely fueled by resurgence in the freshwater regions (Orth *et al.*, 2010). The model indicates an increase over

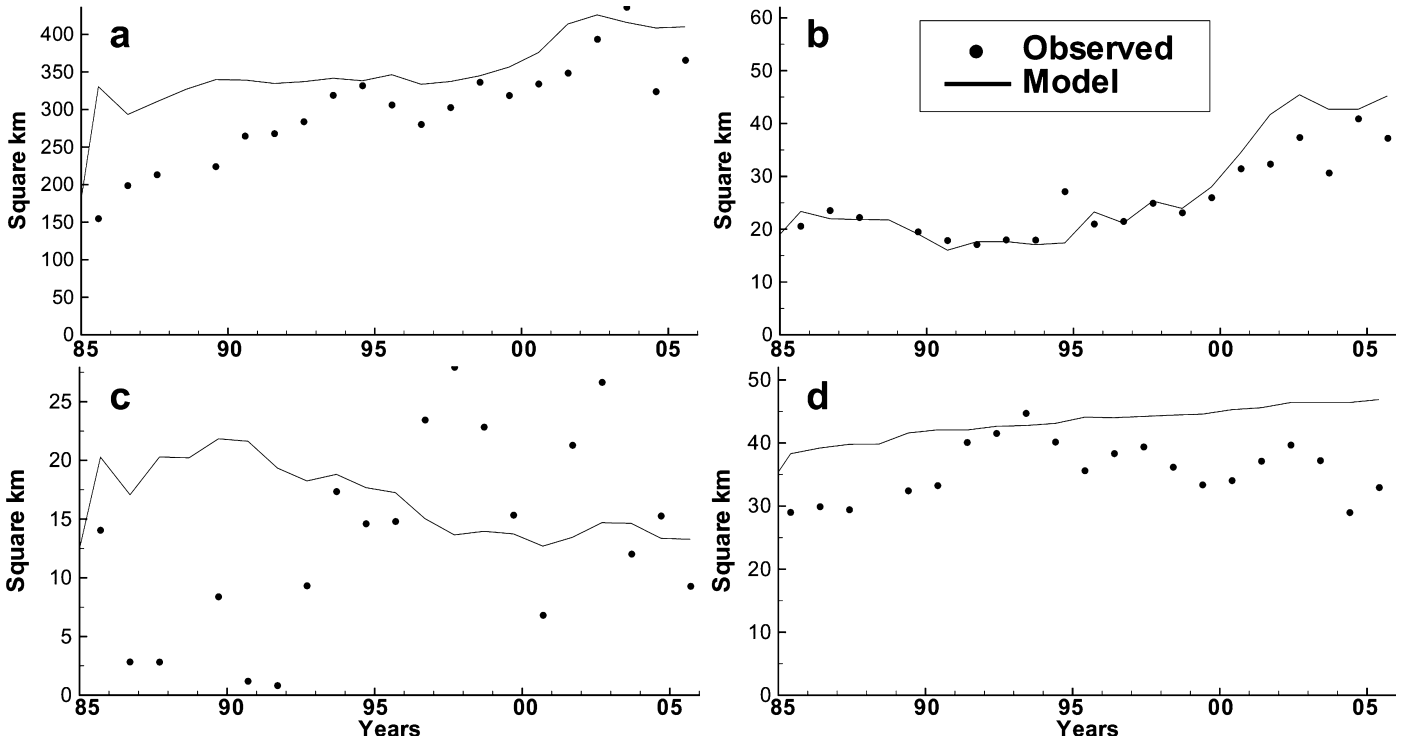

FIGURE 6. Computed and Observed Submerged Aquatic Vegetation Areas 1985-2005. Results are shown for (a) system-wide summary; (b) FRESHWATER community in segment CB1; (c) RUPPIA community in segment CHOMH1; and (d) ZOSTERA community in segment CB7.

this interval as well, although a large fraction of the increase occurs in the first season of operation, between model initiation in January 1985 and late summer when the overflights take place (Figure 6). Observed and computed SAV areas in individual CBPS range over three orders of magnitude (Figure 7). Greatest relative differences between computed and observed are at the lowest ends of the scales. Although positive and negative discrepancies occur, the computed area exceeds observed area in 74% of the comparisons. Modeled area exceeds observed by a median value of 49%.

The "probability" feature of the model allows for high degree of accuracy in reproducing the observed trend in area in the FRESHWATER community (Figure 6b). Probability of success was increased in this region throughout the simulation, from 0.2 to 1.0. The increasing value of probability reflects a community in which the probability of SAV spreading to non-vegetated regions increases as SAV becomes established. The long-term observations in the RUPPIA community (Figure 6c) indicate sporadic behavior with no distinct trend. The model does not reproduce the observed behavior and bears little resemblance to annual surveyed area. The probability concept provides no benefit here. Observed ZOSTERA area oscillates with a small net gain over the duration of the simulation (Figure 6d). The model, with assigned $p = 0.3$, correctly represents the long-term trend, but not the inter-annual oscillations in area. Overall, the computed ZOSTERA area exceeds observed.

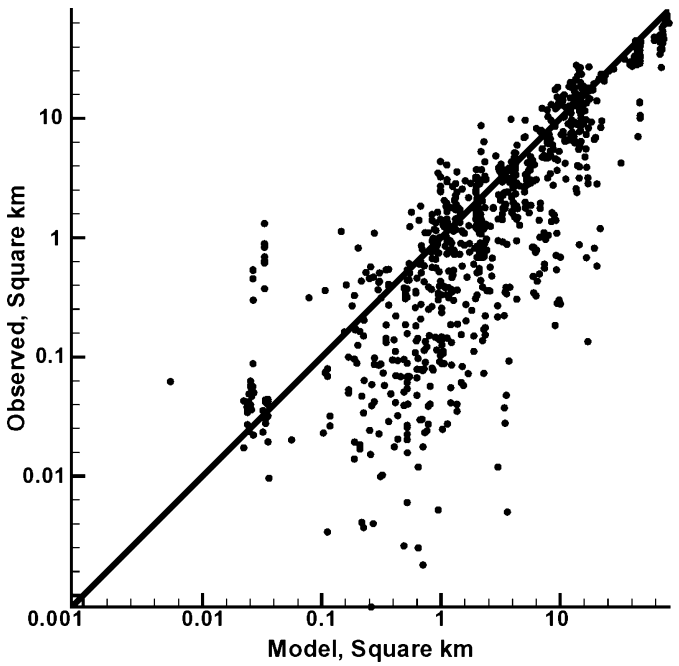

FIGURE 7. Observed and Computed Submerged Aquatic Vegetation (SAV) Area in Individual Chesapeake Bay Program Segments (CBPS). Each point indicates SAV area in a CBPS in one annual survey, ≈850 individual comparisons.

In its present configuration, the SAV model reproduces the order of magnitude of SAV area within CBPS. Inter-annual variability and long-term trends are not universally reproduced. Good results can be obtained through the probability feature although this feature provides little predictive capability. The SAV sub-model is retained in the larger model to provide first-order estimates of interaction between SAV and the surrounding environment, especially the effect of SAV in damping suspended solids resuspension (Cerco *et al.*, 2012). At present, however, attainment of water quality criteria in shallow-water bay grass designated use regions is determined from computations of Ke rather than computed SAV area.

Shallow-Water Light Attenuation

Mean values of light attenuation at the 34 shallow-deep water station pairs were compared using a one-sided *t*-test (Table 1). Results were classified as "significantly different" ($p < 0.01$), "marginally different" ($0.01 < p < 0.05$), and "no difference" ($p < 0.05$). Roughly half the time, no difference was apparent between shallow- and deep-water attenuation. When differences were detected (significant or marginal) shallow-water attenuation exceeded deep-water attenuation in ≈70% of the cases.

TABLE 1. Summary of Observed Deep- and Shallow-Water Station Pairs.

Number of station pairs	34
Number of significantly different pairs ($p < 0.01$)	11
Number of marginally different pairs ($0.01 < p < 0.05$)	6
Number of pairs in which shallow-water Ke significantly exceeds deep-water Ke	7
Number of pairs in which deep-water Ke significantly exceeds shallow-water Ke	4

Note: Ke, light attenuation.

When the shallow-deep water station pairs were mapped to the computational grid for comparison with the model (Figure 4), the population of available pairs dropped to less than half the original size. Instances occurred in which one or both stations in a pair were off the computational grid. In other instances, both stations were in the same computational cell so no difference could be modeled. These difficulties necessitated occasional adjustments in the determination of the paired stations. The remaining pairs resemble the original population in that few of the observed differences are significant and the difference between deep and shallow water shows no

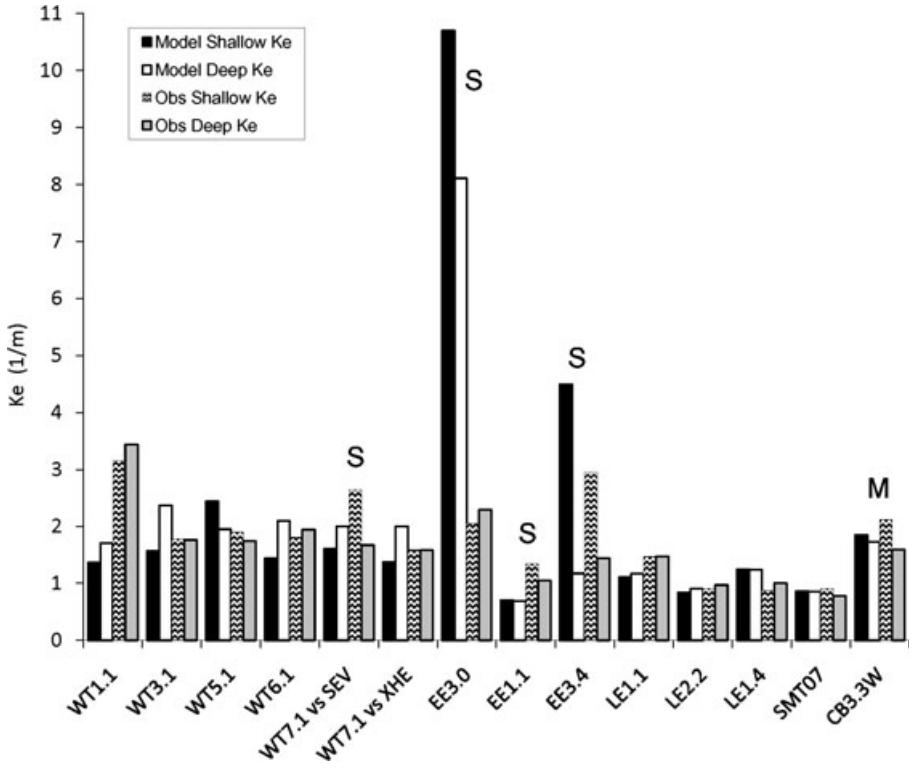

FIGURE 8. Long-Term Average Light Attenuation Measured in Paired Deep- and Shallow-Water Stations. Observed values are from 2002 to 2005. Model values are from 1993 to 1999. "S" indicates deep- and shallow-water observations are significantly different ($p < 0.01$). "M" indicates deep- and shallow-water observations are marginally different ($0.01 < p < 0.05$). As the observations and model are from different periods, the primary purpose of this comparison is to examine computed and observed differences in deep- and shallow-water attenuation.

consistent trend (Figure 8). The model pairs suffer no observational errors. The calculated values and the differences between them are exact. However, the calculated differences cannot be validated against insignificant differences in observations, and the few significantly different observed pairs provide little basis for model validation.

A comprehensive view of model behavior was obtained by comparing computed light attenuation in shallow-water cells with attenuation in remaining cells. Analyses were conducted by CBPS. Daily model computations in each cell were averaged into daily values per CBPS. The contribution of each cell was weighted according to cell surface area. These were averaged across annual SAV growing seasons (April-October) and then averaged up into long-term averages for the period 1993-1999. Shallow-water attenuation exceeds the deep-water value by $\approx 0.1\ m^{-1}$ except for two segments in the upper bay, CB2 and CB3 (Figure 9) where the two values are essentially equal. The reason for the exceptional behavior in these two segments is not apparent although the presence of the persistent turbidity maximum in CB2 may overwhelm the influence of factors that otherwise differentiate shallow and deep water. Sensitivity runs indicate the relative influence of various forcing factors changes with distance from the major inflow. In the upper bay, the loads from the watershed are the major influence on light attenuation (Figure 9). Around CB4, however, and in the two eastern shore embayments considered, the watershed is less influential than bankloads. The solids loads from the major Chesapeake Bay drainage are trapped in the estuarine turbidity maximum which forms upstream of CB4. In the mid bay regions, solids loads from the local watershed are relatively small and of lesser influence than bank erosion. Near the mouth of the bay, where computed attenuation is least, the influences of both loading sources, bankloads and local watershed, are negligible. Segments CB6-7 and CB8 are distant from the primary watershed discharges and contain large expanses of open water relative to the length of shoreline subject to erosion. In most regions considered, the calculated influence of SAV in damping resuspension is of lesser magnitude than the influence of loads.

Individual values of shallow-water attenuation, calculated from the observed vertical profile of irradiance with depth, were compared with model values calculated on the same day. A scatterplot of computed *vs.* observed values shows little correspondence (Figure 10). The results are not surprising. The model cannot reproduce instantaneous measures collected at the extreme reaches of the domain, especially

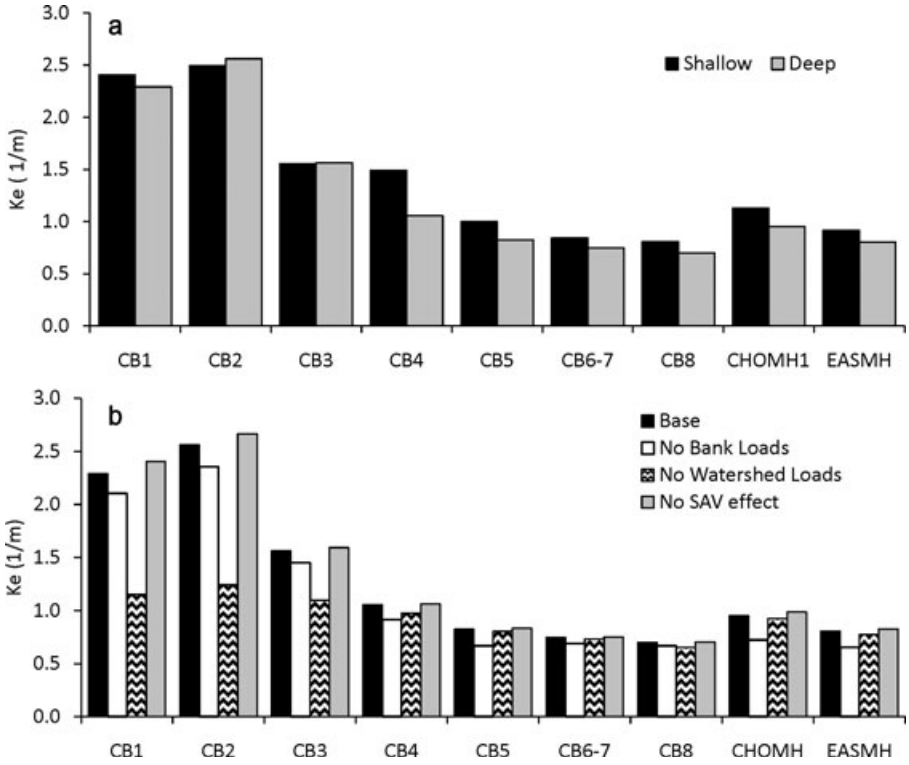

FIGURE 9. (a) Long-Term Average Light Attenuation Computed in Deep *vs.* Shallow Water. (b) Sensitivity of light attenuation (Ke) computed in shallow water to loads from bank erosion, loads from the watershed, and damping of resuspension by submerged aquatic vegetation (SAV). The influences of these factors on deep-water attenuation are similar.

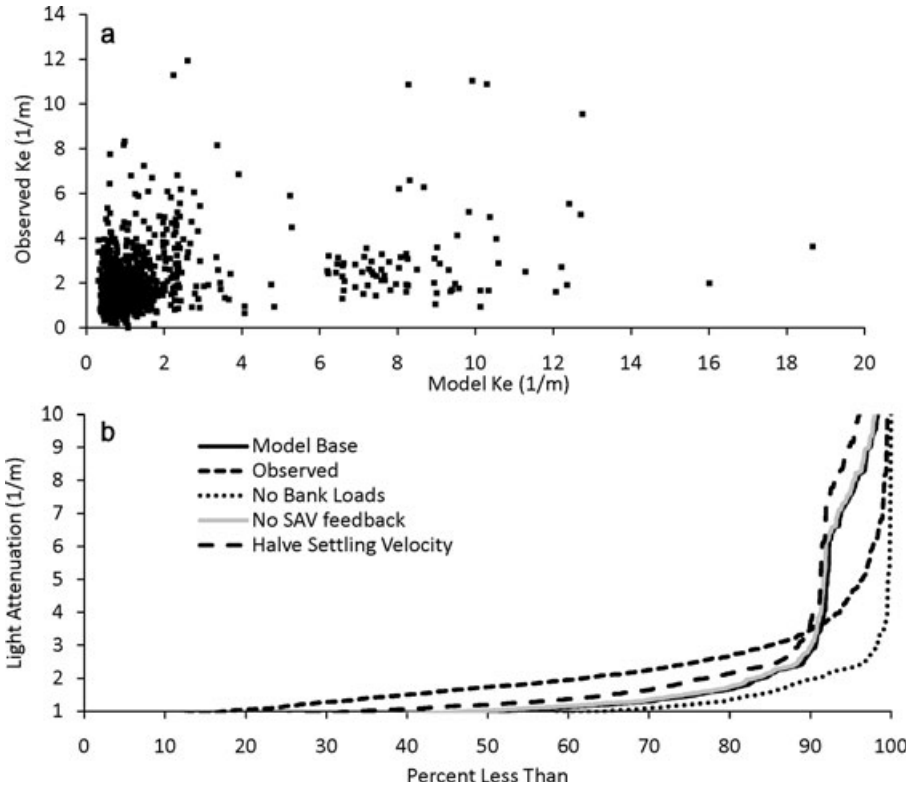

FIGURE 10. Observed and Computed Light Attenuation (Ke) at Shallow-Water Monitoring Stations. Comparisons are shown as (a) scatterplots and (b) cumulative distribution plots. The cumulative distribution plots also show sensitivity of computations to loads from bank erosion, to damping of resuspension by submerged aquatic vegetation (SAV), and to settling velocity.

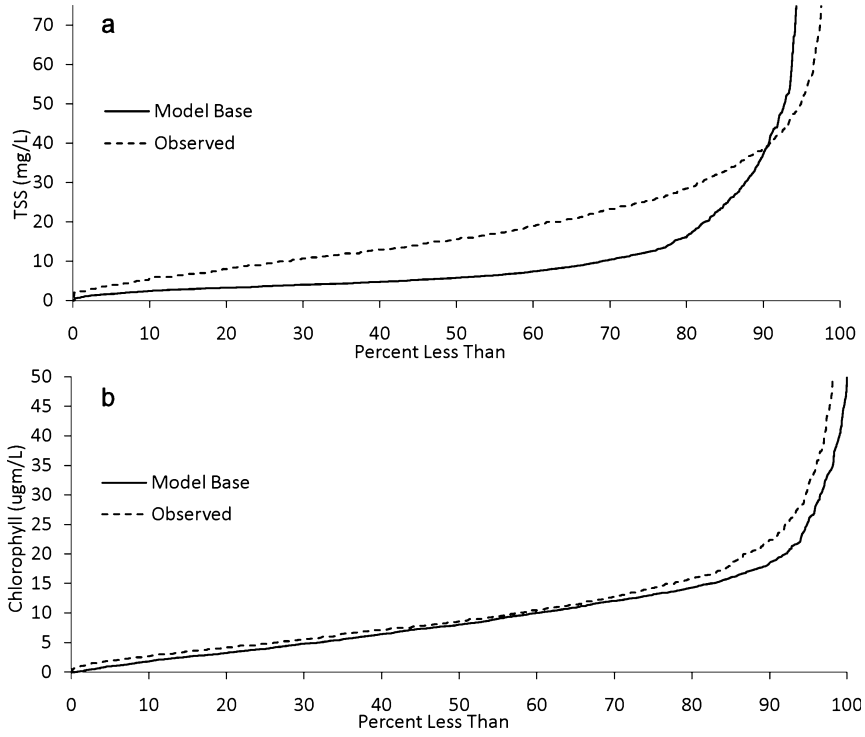

FIGURE 11. Cumulative Distribution Plots of Observed and Computed (a) Total Suspended Solids (TSS) and (b) Chlorophyll at Shallow-Water Monitoring Stations.

when the observed value may be oscillating rapidly (Fluctuations in turbidity measured at 15-min intervals can be viewed at the Maryland DNR Continuous Monitoring web site http://mddnr.chesapeakebay.net/newmontech/contmon/index.cfm). More meaningful comparisons result from cumulative distribution charts which illustrate the extreme and typical values of both observations and model. The distribution of observed values exceeds the modeled values for 90% of the distribution. The median observed value is 1.73 m^{-1} compared to the median modeled value 0.99 m^{-1}. The top 10% of the modeled values exceed observed, however. The predominant excess of observed values over modeled is the opposite of their relative order in open water. There, median modeled attenuation exceeds observed by 0.2 m^{-1} (Cerco and Noel, this issue).

The shortfall in computed Ke reflects a similar shortfall in computed TSS (Figure 11). The total solids analyses do not isolate the organic and inorganic fractions of the total. However, the modeled chlorophyll distribution agrees well with the observed distribution; the modeled median is within 0.6 μg/l of the observed median (Figure 11). Close agreement of the computed and observed chlorophyll suggests that the modeled values of particulate organic matter are representative. Therefore, the solids shortfall is tentatively attributed to the inorganic fraction. Sensitivity runs aimed at exploring the roles of various influences in determining shallow-water attenuation indicate the observed distribution of Ke cannot easily be replicated. The sensitivity runs indicate that the extreme modeled values are the result of bank erosion events. When bank erosion is eliminated, the upper 20% of the modeled distribution falls off substantially. Neither alterations in particle settling velocity nor elimination of SAV damping of particle resuspension raise the preponderance of modeled values to match the observed Ke distribution (Figure 10).

DISCUSSION

SAV Model

The SAV model can be more properly designated an "SAV production model." Production is computed as a function of light, temperature, and nutrient availability. When conditions are favorable, production occurs, with little relationship with antecedent conditions. With this formulation, SAV biomass rapidly equilibrates with the environment. Increases in biomass, which take years to develop in the bay take place almost instantly in the model (Figure 6). The instantaneous increases were slowed but not eliminated through introduction of the "probability of growth" feature. Realistic reproduction of observed trends and forecasting of future trends requires addition of plant propagation to the model. The model must also be revised to account for differences in plant structure and life history. The model as formulated cannot simultaneously replicate the low amplitude, long-period, oscillations in ZOSTERA area, and the sporadic fluctuations in RUPPIA. At present, the model is suited for computing the equilibrium distribution of SAV on a system-wide scale and is more suited for perennial communities, such as ZOSTERA, rather than sporadic communities such as RUPPIA.

Deep vs. *Shallow Water*

The observations indicate no clear, predominant difference or relationship between Ke measured in shallow water and Ke measured in an adjacent channel region. This issue has been examined previously and summarized recently (USEPA, 2003). Distance between the paired stations appears to be the predominant factor that determines similarity or difference in Ke. Stations separated by less than 2 km are likely to demonstrate similar Ke relative to SAV habitat criteria. No doubt, differences in deep-water attenuation and nearby shallow-water attenuation are attributable to both deterministic, physical processes, and to shortfalls in number and quality of observations. Observational errors do not affect model analyses. Long-term, regional summaries indicate computed shallow-water Ke exceeds observed in much of Chesapeake Bay and adjacent embayments. Model sensitivity analyses indicate the influences on computed Ke vary regionally. Loads from the watershed are the predominant influence in the upper bay (CB1-CB3) while bank erosion is of greater influence in the lower bay and embayments. The dominant role of the watershed loads may be responsible for the lesser difference in deep- *vs.* shallow-water Ke in two upper bay CBPS, CB2 and CB3, compared to segments further downstream from the major watershed discharge.

Shallow-Water Light Attenuation

The model was compared to a set of ≈1,000 shallow-water light attenuation measurements collected primarily in eastern shore tributaries. The model exhibits a shortfall in computed Ke; the median modeled value is ≈0.7 m^{-1} less than observed. This result is in contrast to open water where the

median model Ke exceeds observed. While multiple factors potentially influence the shortfall in modeled Ke, a concurrent shortfall in computed TSS identifies suspended solids dynamics as the leading process for investigation. Sensitivity analysis indicates the observed Ke distribution cannot be readily replicated through adjustment of model parameters and inputs. A potential problem exists in the model computation of wave-generated bottom shear stress. The present model considers fetch-limited waves (Cerco *et al.*, 2010). In the convoluted tributaries, fetch is short and computed stress is negligible. In reality, refraction may propagate waves into regions where local generation is absent and produce shear stress which is not modeled. A second issue is the potential influence of distinctive shallow-water processes which are absent from the model. These processes include biotic effects on solids dynamics (Passow, 2002) and solids production through precipitation of iron oxyhydroxides (Bricker *et al.*, 2004). Research and additional measurements are required to improve computations of Ke in these shallow regions.

Recommendations for Model Development

The shallow-water component of the CBEMP largely represents an extension of existing model algorithms into previously de-emphasized portions of the model domain. The most rigorous examination of the model performance involves the comparison with observations collected in the shallow-water monitoring program 2000-2005 (Figures 10 and 11). These indicate model performance in computation of TSS and Ke is distinctly different from model performance in the deep, open waters of the bay. The geographic extent of the observations is limited, however (Figure 4), and conclusions regarding model performance are tentative. The next step in model development is extension of the time period to 2011, to incorporate additional shallow-water observations in widespread regions of the bay. The additional comparisons provided by the extension of the application period will provide expanded insight into model performance and into the generality of the results obtained with data collected largely on the eastern shore. Subsequently, decisions can be made regarding the necessity and nature of further model improvements. The present structured computational grid of quadrilateral elements is reaching the limits of resolution relative to the convoluted geometry of the nearshore region. A desire for increased resolution will likely require a switch to a specialized, shallow-water model based on a different grid conception, e.g., an unstructured mesh of triangular elements (Chen *et al.*, 2006; Martin *et al.*, 2011) to improve fit between the model domain and the environment. The benefits obtained from increased resolution alone, however, may not be fruitful without concurrent investigation into processes which determine solids dynamics and light attenuation in shallow water.

The role of the present SAV model is to provide feedback between SAV and sediment resuspension. The model is capable of computing the extent of larger SAV beds and is useful in computing the maximum extent of SAV change expected as a result of management actions. The trajectory from existing to future conditions is unpredictable, however, as is the inter-annual variation in sporadic SAV species. More accurate prediction of SAV biomass and area requires a revised model. Incorporation of reproduction and propagation are recommended as first steps. Additional model complexity beyond these steps will be difficult to implement on a system-wide scale, largely due to data limitations, although improved model capability in localized, well-monitored areas may be possible. As with the physical aspects of the shallow-water environment, model improvements alone will not be sufficient. The SAV beds in the upper bay are presently undergoing an unprecedented recovery (Orth *et al.*, 2010) which is not entirely explained by existing paradigms. A combination of both process-based investigation and model improvements is required for development of a fully predictive SAV model.

ACKNOWLEDGMENTS

This study was funded by the US Army Engineer District, Baltimore, and by the US Environmental Protection Agency Chesapeake Bay Program Office. The optical model was contributed by Dr. Charles Gallegos of the Smithsonian Environmental Research Center. US Environmental Protection Agency publication EPA-903-R-13-009, Chesapeake Bay Program publication CBP/TRS-315-13-8.

LITERATURE CITED

Bricker, O., W. Newell, and N. Simon, 2004. Bog Iron Formation in the Nassawango Creek Watershed, Maryland, USA. *In:* First International Conference on Monitoring, Management, Simulation and Remediation of the Geological Environment (GeoEnvironment), Segovia, Spain, J. Martin-Deque, C. Brebbia, A. Godfrey, and J. Diaz de Teran (Editors). WIT Press, Southampton, United Kingdom, pp. 13-23, ISBN: 0-85312-723-X.

Cerco, C. and T. Cole, 1993. Three-Dimensional Eutrophication Model of Chesapeake Bay. Journal of Environmental Engineering 119(6):1006-1025.

Cerco, C., S.-C. Kim, and M. Noel, 2010. The 2010 Chesapeake Bay Eutrophication Model. A Report to the US Environmental Protection Agency Chesapeake Bay Program and to the US Army Engineer Baltimore District. http://www.chesapeakebay.net/publications/title/the_2010_chesapeake_bay_eutrophication_model1, *accessed* July 2013.

Cerco, C., S.-C. Kim, and M. Noel, 2012. Management Model of Suspended Solids in the Chesapeake Bay, USA. Estuarine, Coastal, and Shelf Science 116:87-98, doi: 10.1016/j.ecss.2012.07.009.

Cerco, C. and K. Moore, 2001. System-Wide Submerged Aquatic Vegetation Model for Chesapeake Bay. Estuaries 24(4):522-534.

Cerco, C. and M. Noel, 2004. The 2002 Chesapeake Bay Eutrophication Model. US Environmental Protection Agency Chesapeake Bay Program Office EPA 903-R-04-004, 349 pp. http://www.chesapeakebay.net/publications/title/the_2002_chesapeake_bay_eutrophication_model, *accessed* July 2013.

Cerco, C. and M. Noel, 2007. Can Oyster Restoration Reverse Cultural Eutrophication in Chesapeake Bay? Estuaries and Coasts 30(2):331-343.

Cerco, C. and M. Noel, 2010. Monitoring, Modeling, and Management Impacts of Bivalve Filter Feeders in the Oligohaline and Tidal Fresh Regions of the Chesapeake Bay System. Ecological Modelling 221:1054-1064.

Cerco, C., M. Noel, and L. Linker, 2004. Managing for Water Clarity in Chesapeake Bay. Journal of Environmental Engineering 130(6):631-642.

Cerco, C.F. and M.R. Noel, this issue. Twenty-One-Year Simulation of Chesapeake Bay Water Quality Using the CE-QUAL-ICM Eutrophication Model. Journal of the American Water Resources Association, doi: 10.1111/jawr.12107. EPA-903-R-13-011. CBP/TRS-317-13-10.

Chen, C., R.C. Beardsley, and G. Cowles, 2006. An Unstructured Grid, Finite-Volume Coastal Ocean Model (FVCOM) System. Oceanography 19(1):78-89.

Chesapeake Bay Program, 1992. Submerged Aquatic Vegetation Habitat Requirements and Restoration Targets: A Technical Synthesis. CBP/TRS 83/92. US Environmental Protection Agency Chesapeake Bay Program, Annapolis, Maryland, 186 pp.

DiToro, D., 2001. Sediment Flux Modeling. John Wiley and Sons, New York City, New York, ISBN: 0-471-13535-6.

Gallegos, C., 2001. Calculating Optical Water Quality Targets to Restore and Protect Submerged Aquatic Vegetation: Overcoming Problems in Partitioning the Diffuse Attenuation Coefficient for Photosynthetically Active Radiation. Estuaries 24(3):381-397.

Gallegos, C., E. Lewis, and H. Kim, 2006. Coupling Suspended Sediment Dynamics and Light Penetration in Chesapeake Bay. http://www.chesapeakebay.net/publications/title/coupling_suspended_sediment_dynamics_and_light_penetration_in_the_upper_che, *accessed* July 2013.

Gallegos, C.L., P.J. Werdell, and C.R. McClain, 2011. Long-Term Changes in Light Scattering in Chesapeake Bay Inferred From Secchi Depth, Light Attenuation, and Remote Sensing Measurements. Journal of Geophysical Research 117:1-19, doi: 10.1029/JC2011007160.

Holmes, R., 1970. The Secchi Disk in Turbid Coastal Water. Limnology and Oceanography 15:688-694.

Johnson, B., K. Kim, R. Heath, B. Hsieh, and L. Butler, 1993. Validation of a Three-Dimensional Hydrodynamic Model of Chesapeake Bay. Journal of Hydraulic Engineering 199(1):2-10.

Kim, S.-C., this issue. Evaluation of a Three-Dimensional Hydrodynamic Model Applied to Chesapeake Bay Through Long-Term Simulation of Transport Processes. Journal of the American Water Resources Association, doi: 10.1111/jawr.12113. EPA-903-R-13-006. CBP/TRS-312-13-5.

Lee, Z.-P., K.P. Du, and R. Arnone, 2005. A Model for the Diffuse Attenuation Coefficient of Downwelling Irradiance. Journal of Geophysical Research 110:1-10, doi: 10.1029/2004JC002275.

Martin, S.K., G. Savant, and D. McVan, 2011. Two Dimensional Numerical Model of the Gulf Intracoastal Waterway Near New Orleans. ASCE Journal of Waterway, Port, Coastal, and Ocean Engineering 138(3):236-245, doi: 10.1061/(ASCE)WW.1943-5460.0000119.

Moore, K., D. Wilcox, and R. Orth, 2000. Analysis of the Abundance of Submersed Aquatic Vegetation Communities in the Chesapeake Bay. Estuaries 23:115-127.

Orth, R.J., M. Williams, S. Marion, D. Wilcox, T. Carruthers, W. Kenneth Moore, M. Kemp, W. Dennison, N. Rybicki, P. Bergstrom, and R. Batiuk, 2010. Long-Term Trends in Submersed Aquatic Vegetation (SAV) in Chesapeake Bay, USA, Related to Water Quality. Estuaries and Coasts 33(5):1144-1163, doi: 10.1007/s12237-010-9311-4.

Passow, U., 2002. Transparent Exopolymer Particles (TEP) in Aquatic Environments. Progress in Oceanography 55:287-333.

Shenk, G.W. and L.C. Linker, this issue. Development and Application of the 2010 Chesapeake Bay Watershed Total Maximum Daily Load Model. Journal of the American Water Resources Association, doi: 10.1111/jawr.12109. EPA-903-R-13-004. CBP/TRS-310-13-3.

USEPA (U.S. Environmental Protection Agency), 2003. Ambient Water Quality Criteria for Dissolved Oxygen, Water Clarity and Chlorophyll a for the Chesapeake Bay and Its Tidal Tributaries. EPA 903-R-03-002. U.S. Environmental Protection Agency Region III Chesapeake Bay Program Office, Annapolis, Maryland, 343 pp. http://www.chesapeakebay.net/publications/title/ambient_water_quality_criteria_for_dissolved_oxygen_water_clarity_and_chlor, *accessed* July 2013.

USEPA (U.S. Environmental Protection Agency), 2008. Ambient Water Quality Criteria for Dissolved Oxygen, Water Clarity and Chlorophyll a for the Chesapeake Bay and Its Tidal Tributaries. 2008 Technical Support for Criteria Assessment Protocols Addendum. EPA 903-R-08-001. U.S. Environmental Protection Agency Region III Chesapeake Bay Program Office, Annapolis, Maryland, 82 pp. http://www.chesapeakebay.net/publications/title/ambient_water_quality_criteria_for_dissolved_oxygen_water_clarity_and_3, *accessed* July 2013.